Journal of Harbin Engineering University
ISSN: 1006-7043

Vol 44 No. 12
December 2023

Heat Generation Effects on Couple Stress Fluid over a Deformable Surface with Aluminium Alloy Nanoparticles

Iskandar Waini [1], Khairum bin Hamzah [2], Farah Nadzirah Jamrus [3], Anuar Ishak [4], Ioan Pop [5]

[1, 2] Fakulti Teknologi dan Kejuruteraan Industri dan Pembuatan, Universiti Teknikal Malaysia Melaka, Hang Tuah Jaya, Durian Tunggal 76100, Melaka, Malaysia

[3] Kolej Pengajian Pengkomputeran, Informatik dan Matematik, Universiti Teknologi MARA (UiTM) Cawangan Melaka Kampus Jasin, 77300 Merlimau, Melaka, Malaysia

[4] Department of Mathematical Sciences, Faculty of Science and Technology, Universiti Kebangsaan Malaysia, 43600 UKM, Bangi, Selangor, Malaysia

[5] Department of Mathematics, Babes-Bolyai University, Romania

Abstract

In the current research, a mathematical analysis of couple stress fluid flow and heat characteristics through a deformable surface with hybrid nanoparticles and heat generation effects is conducted. The solid nanoparticles of the aluminium alloys (AA7072 and AA7075) are suspended in methanol to create the hybrid nanofluid. The similarity approach is used to reduce the governing equations into the similarity equations. Then, MATLAB's bvp4c function is employed to solve the resulting equations. The solutions for the flow and temperature fields, as well as the skin friction coefficient and Nusselt number are presented in table and graphical forms. The results demonstrate that hybrid nanofluids excel as thermal conductors, significantly augmenting the heat transfer rate. The heat transfer rate is increased by 0.78% with 2% of added hybrid nanoparticles if compared to the base fluid. Furthermore, the heat generation contributes to the enhancement of the fluid temperature by thickening the thermal boundary layer. This led to the reduction of the heat transfer rate of the hybrid nanofluid.

Keywords: Couple Stress Fluid, Hybrid Nanofluid, Shrinking Sheet, Heat Generation.

1. Introduction

In recent years, there has been a notable surge in the interest of researchers and scientists towards the advancement of heat transfer fluids. While conventional fluids widespread use in engineering and industrial applications, their heat transfer capabilities are limited due to their low thermal conductivity. To overcome this limitation, researchers introduced a solution known as 'nanofluid' in 1995, pioneered by Choi and Eastman [1]. This innovative approach involves incorporating nanosized particles into the aforementioned fluids. Then, Khanafer et al. [2], and Oztop and Abu-Nada [3] studied the nanofluid flow in a rectangular enclosure. However, in order to further enhance the thermal properties of nanofluids, researchers have developed a novel type of fluid known as 'hybrid nanofluid'. Early studies focusing on the utilization of hybrid nano-composite particles can be attributed to Jana et al. [4]. Unlike conventional nanofluids, hybrid nanofluids consist of multiple types of nanoparticles, which synergistically enhance the heat transfer rate [5,6]. By combining or hybridizing appropriate nanoparticles, the desired level of heat transfer can be achieved, see Suresh et al. [7]. Takabi and Salehi [8] conducted a study on enhancing the heat transfer efficiency of a sinusoidal corrugated enclosure using a hybrid nanofluid. Numerous papers on hybrid nanofluids have been published and are accessible in the literature, see Refs [9–13].

The theory of couple stress fluids serve as an extension of the classical Newtonian fluids, allowing for the inclusion of polar effects such as body couples and couple stresses, see Stokes [14]. Couple stress

fluids find practical applications in various fields, including biomechanics, chemical and petroleum industries, geothermal energy extraction, geohydrology, and medicine. Several researchers have conducted simulations and investigations pertaining to couple stress flows in different contexts. For instance, Turkyilmazoglu [15] investigated the flow and heat characteristics of couple stress fluid over surfaces that can stretch or shrink. Khan et al. [16] computationally studied flow of couple stress with several surface temperature conditions. Additionally, Das et al. [17] reported the effects of the Darcy-Forchheimer on couple stress fluid past an inclined sheet.

The industrial sector has a range of applications for heat generation effects, including electrification of industrial process heat, solar thermal systems for industrial process heat in tropical climates, and the integration of solar process heat in various industries. Understanding the impact of heat generation is essential for optimizing the design and performance of these systems, and also improve the energy efficiency (Wahed et al., [18], Schüwer and Schneider [19], Tasmin et al., [20]. Additionally, the review by Liu et al. [21] highlights the importance of reducing heat generation in rubber composites to enhance their performance. Moreover, Makinde and Olanrewaju [22] explored the combined effects of internal heat generation and buoyancy force on boundary layer flow, observing an overshot of fluid velocity and thickening of the thermal boundary layer. Khan et al. [23] explored the impact of heat generation on the flow of Maxwell fluid. Ojjela et al. [24] considering the effects of the heat generation in an expanding channel. There are several studies collectively highlight the complex and multifaceted nature of the relationship between heat generation and boundary layer flow as reported in Ibrahim and Gadisa [25], Goud [26], and Adeniyan et al. [27].

In recent times, numerous types of nanomaterial have been reported in the literature. Notably, aluminum alloy nanoparticles AA7075 and AA7072 stand out as exceptional nanomaterials due to their remarkable thermal, chemical, and physical properties, see Tlili [28]. The special features and superior properties make them highly desirable for various industrial applications, including aerospace. Also, these alloys find extensive applications in the manufacturing of transportation equipment such as glider aircraft and rocket frames [28]. Different from the previous study of Turkyilmazoglu [15], the objective of this endeavor is to investigate the effects of hybrid nanoparticles over a stretched surface in a couple stress fluid. The hybrid nanoparticles considered in this study are aluminum alloy nanoparticles AA7075 and AA7072, while the base fluid is methanol. The obtained results are presented in graphical and tabular forms for several physical parameters. It should be mentioned that this problem has not been explored. Hence, this study holds immense importance as a future point of reference for practitioners, scientists, engineers, and fluid mechanists.

2. Mathematical formulation

In this study, we examine the behavior of an electrically conducting quiescent couple stress fluid interacting with a deformable surface. We consider the influence of hybrid nanoparticles and a uniform external magnetic field, with the coordinates *x* and *y* denoting the surface and normal directions, respectively. Additionally, the volumetric heat generation δ_0 in the energy equation. Here, the velocity and temperature at the wall are taken as $u_w(x) = ax$ and $T_w(x) = T_\infty + T_0 x^2$, respectively.

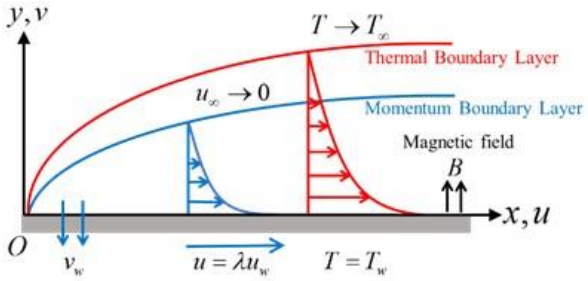

Fig. 1. Schematic Model

The governing equations are then given by, see Turkyilmazoglu [15]

$$u_x + v_y = 0 \quad (1)$$

$$uu_x + vu_y = \frac{\mu_{hnf}}{\rho_{hnf}} u_{yy} - \frac{\eta_0}{\rho_{hnf}} u_{yyy} - \frac{\sigma_{hnf}}{\rho_{hnf}} B_0^2 u \quad (2)$$

$$uT_x + vT_y = \frac{k_{hnf}}{(\rho c_p)_{hnf}} T_{yy} + \frac{\delta_0}{(\rho c_p)_{hnf}} (T - T_\infty) \quad (3)$$

subject to:

$$v = v_w,\ u = \lambda u_w = \lambda a x,\ T = T_w = T_\infty + T_0 x^2 \text{ at } y = 0$$

$$u \to 0,\ u_y \to 0,\ u_{yy} \to 0,\ T \to T_\infty \text{ as } y \to \infty \quad (4)$$

where η_0 is the material constant for the couple stress fluid, ρ is the density, and μ is the dynamic viscosity. The properties of hybrid nanofluid are given in Tables I and II. The following similarity transformations are considered, see Turkyilmazoglu [15].

$$\psi = x\sqrt{av_f}f(\eta), u = axf'(\eta), v = -\sqrt{av_f}f(\eta),$$

$$\theta(\eta) = \frac{T-T_\infty}{T_w-T_\infty}, \eta = y\sqrt{\frac{a}{v_f}} \quad (5)$$

Here, ψ signifies the stream function with $u = \partial\psi/\partial y$ and $v = -\partial\psi/\partial x$ which satisfied (1). Then, using (5), the governing equations (2) and (3) are reduced to the similarity form

$$-Cf'''' + \frac{\mu_{hnf}/\mu_f}{\rho_{hnf}/\rho_f}f''' + ff'' - f'^2 - \frac{\sigma_{hnf}/\sigma_f}{\rho_{hnf}/\rho_f}Mf' = 0 \quad (6)$$

$$\frac{1}{Pr}\frac{k_{hnf}/k_f}{(\rho C_p)_{hnf}/(\rho C_p)_f}\theta'' + f\theta' - 2f'\theta + \frac{1}{(\rho C_p)_{hnf}/(\rho C_p)_f}\delta\theta = 0 \quad (7)$$

subject to:

$$f(0) = S, f'(0) = \lambda, \theta(0) = 1, \quad (8)$$

$f'(\eta) \to 0$, $f''(\eta) \to 0$, $f''''(\eta) \to 0$, $\theta(\eta) \to 0$ as $\eta \to \infty$

with $\lambda = 1$ and $\lambda = -1$ represent the stretching and shrinking parameters, respectively. Further, Prandtl number Pr, the mass flux parameter *S*, the couple stress parameter *C*, the magnetic parameter *M*, and the heat source/sink parameter δ are defined as

$$\Pr = \frac{(\mu C_p)_f}{k_f}, S = -\frac{v_w}{\sqrt{av_f}}, C = \frac{\eta_0 a}{\rho_{hnf}v_f^2}, \quad (9)$$

$$M = \frac{\sigma_f B_0^2}{a\rho_f}, \delta = \frac{\delta_0}{a(\rho C_p)_f}$$

Here, $\delta > 0$ and $\delta < 0$ signify the heat source and heat sink, respectively. The local Nusselt number Nu_x and the skin friction coefficient C_f are given as

$$Nu_x = \frac{xq_w}{k_f(T_w-T_\infty)}, C_f = \frac{\tau_w}{\rho_f u_w^2} \quad (10)$$

where the surface heat flux and the surface shear stress are defined by

$$q_w = -k_{hnf}\left(\frac{\partial T}{\partial y}\right)_{y=0}, \tau_w = \mu_{hnf}\left(\frac{\partial u}{\partial y}\right)_{y=0} \quad (11)$$

Thus, we have:

$$Re_x^{-1/2}Nu_x = -\frac{k_{hnf}}{k_f}\theta'(0), Re_x^{1/2}C_f = \frac{\mu_{hnf}}{\mu_f}f''(0) \quad 12)$$

where $Re_x = u_w x/v_f$ denote the local Reynolds number.

Table I The properties of AA7075, AA7072, and methanol [28]

Properties	Nanoparticles		Base fluid
	AA7075	**AA7072**	**Methanol**
$\rho\ (kg/m^3)$	2810	2720	792
$C_p\ (J/kgK)$	960	893	2545
$k\ (W/mK)$	173	222	0.2035
$\sigma\ (S/m)$	26.77×10^6	34.83×10^6	0.5×10^{-6}
Prandtl number, Pr			7.38

Table II The thermophysical properties of hybrid nanofluid [10]

Thermophysical properties	Hybrid Nanofluid
Dynamic viscosity	$\boldsymbol{\mu_{hnf} = \frac{\mu_f}{(1-\phi_{hnf})^{2.5}}}$
Heat capacity	$\boldsymbol{(\rho C_p)_{hnf} = (1-\phi_{hnf})(\rho C_p)_f + \phi_1(\rho C_p)_{n1} + \phi_2(\rho C_p)_{n2}}$
Density	$\boldsymbol{\rho_{hnf} = (1-\phi_{hnf})\rho_f + \phi_1\rho_{n1} + \phi_2\rho_{n2}}$

Thermal conductivity	$\frac{k_{hnf}}{k_f} = \frac{\frac{\phi_1 k_{n1} + \phi_2 k_{n2}}{\phi_{hnf}} + 2k_f + 2(\phi_1 k_{n1} + \phi_2 k_{n2}) - 2\phi_{hnf} k_f}{\frac{\phi_1 k_{n1} + \phi_2 k_{n2}}{\phi_{hnf}} + 2k_f - (\phi_1 k_{n1} + \phi_2 k_{n2}) + \phi_{hnf} k_f}$
Electric conductivity	$\frac{\sigma_{hnf}}{\sigma_f} = \frac{\frac{\phi_1 \sigma_{n1} + \phi_2 \sigma_{n2}}{\phi_{hnf}} + 2\sigma_f + 2(\phi_1 \sigma_{n1} + \phi_2 \sigma_{n2}) - 2\phi_{hnf} \sigma_f}{\frac{\phi_1 \sigma_{n1} + \phi_2 \sigma_{n2}}{\phi_{hnf}} + 2\sigma_f - (\phi_1 \sigma_{n1} + \phi_2 \sigma_{n2}) + \phi_{hnf} \sigma_f}$

3. Results and discussion

This section presents a comprehensive analysis of the numerical results obtained from solving (6)-(8) using the MATLAB software's bvp4c package [29]. Detailed discussions are provided regarding the impact of various physical parameters associated with the proposed model. The values of the parameters are referred from the previous study, see Turkyilmazoglu [15]. For the limiting cases, the models of Turkyilmazoglu [15] are equivalent to the present model. The validation processes yielded excellent agreement across all aspects, demonstrating a high level of consistency, see Table III.

The variations of $Re_x^{1/2} C_f$ and $Re_x^{-1/2} Nu_x$ against ϕ_{hnf} and M are presented in Figs. 2 and 3. The increasing values of M tend to decline the values of $Re_x^{1/2} C_f$ and $Re_x^{-1/2} Nu_x$. However, the values of these physical quantities are enhanced with the rising of ϕ_{hnf} and their values are intensified when

ϕ_{hnf} become larger. This finding supports the notion that hybrid nanofluids exhibit superior thermal characteristics owing to the synergistic effects observed.

Fig. 4 shows the variations of $Re_x^{-1/2} Nu_x$ with ϕ_{hnf} and δ. Note that the heat transfer rate is decreased with the increasing of δ. An interesting observation are noted on the heat transfer rate for the simultaneous effects of the nanoparticles and heat generation. The rates are occurred almost at the same value for $\delta = 0$ where there is no heat generation is considered. Meanwhile, the rates are enhanced as ϕ_{hnf} increase for the case of heat sink ($\delta < 0$). However, an opposing effect observed for the case of heat source ($\delta > 0$) where the rates are declined when ϕ_{hnf} is increased. Additionally, the numerical values of $Re_x^{-1/2} Nu_x$which corresponded to Fig. 4 is given in Table IV. For fixed value of $\delta = -1$, the heat transfer rate is increased by 0.78% for $\phi_{hnf} = 2\%$ and 1.61% for $\phi_{hnf} = 4\%$ if compared to $\phi_{hnf} = 0\%$ (regular fluid).

Table III Values of $-f''(0)$ and $-\theta'(0)$ for various values of M when $C = 0.01, \delta = \phi_1 = \phi_2 = 0, S = 2, Pr = 1$, and $\lambda = -1$

M	**Turkyilmazoglu** [15] **(Exact Solution)**		**Present results (bvp4c)**	
	$-f''(0)$	$-q'(0)$	$-f''(0)$	$-q'(0)$
0	8.87298335	1.71880075	8.87298335	1.71880075
1	8.78885066	1.71651765	8.78885066	1.71651766
3	8.60576725	1.71141583	8.60576725	1.71141583
6	8.27949145	1.70184151	8.27949146	1.70184151

Table IV Values of $Re_x^{-1/2}Nu_x$ for various values of δ and ϕ_{hnf} when $C = 0.01, M = 0, S = 1, Pr = 7.38$, and $\lambda = -1$

δ	$\phi_{hnf} = 0\%$ $(\phi_1 = \phi_2 = 0)$	$\phi_{hnf} = 2\%$ $(\phi_1 = \phi_2 = 0.01)$	$\phi_{hnf} = 4\%$ $(\phi_1 = \phi_2 = 0.02)$
-1	7.06313126	7.11842111	7.17699821
-0.5	6.55643348	6.58842951	6.62355862
0	5.97289576	5.97511385	5.98008739
0.5	5.26598501	5.22531073	5.18618436
1	4.31237285	4.19028745	4.06353662

Fig. 5 illustrates the impact of the heat generation parameter, δ on the temperature field. The increasing value of δ improving the temperature profiles. Separately, it is noted that the temperature profiles are declining for the heat sink case $(\delta < 0)$ and opposing effect observed for the heat source case $(\delta > 0)$. Physically, a higher heat generation parameter leads to increased heat production, thereby augmenting the temperature field. Meanwhile, the heat sink helps in reducing the temperature within the boundary layer by absorbing the heat.

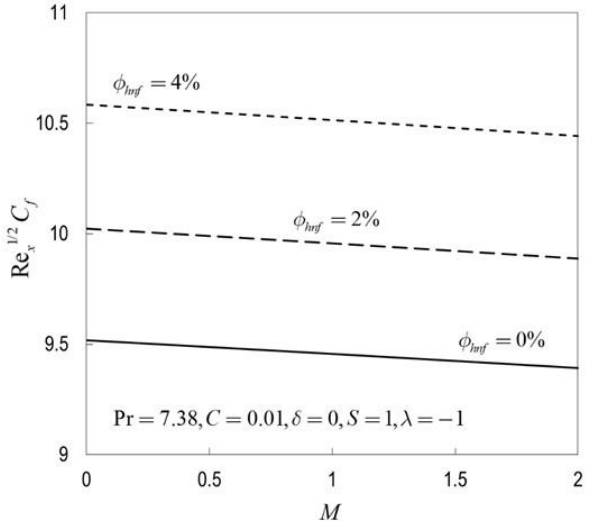

Fig. 2. Variations of $Re_x^{1/2}C_f$ with ϕ_{hnf} and M

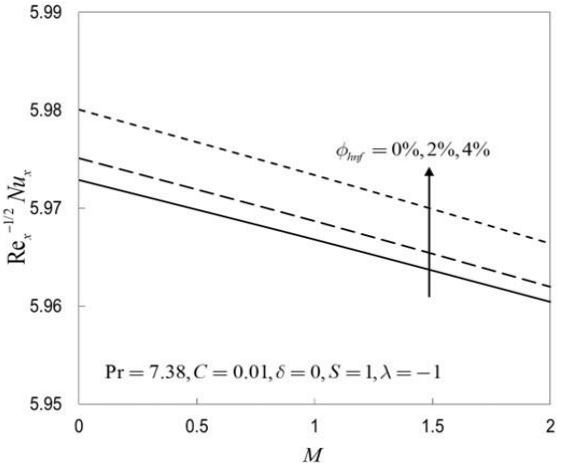

Fig. 3. Variations of $Re_x^{-1/2}Nu_x$ with ϕ_{hnf} and M

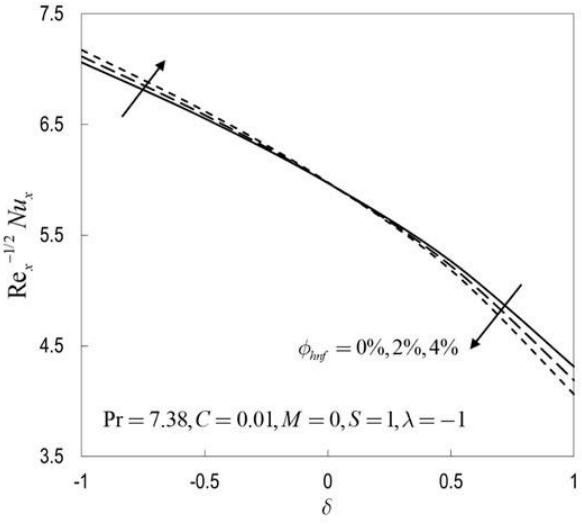

Fig. 4. Variations of $Re_x^{-1/2}Nu_x$ with ϕ_{hnf} and δ

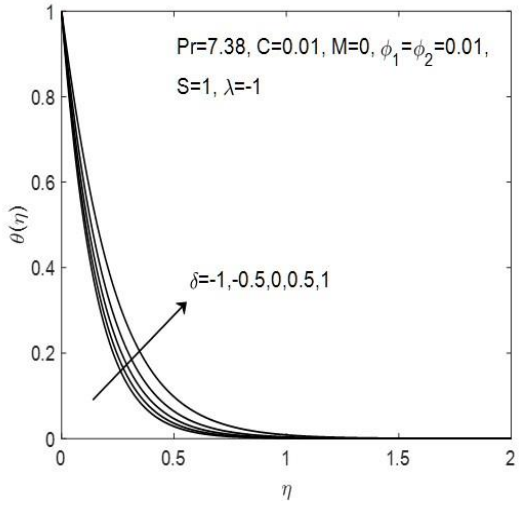

Fig. 5. Temperature profiles $\theta(\eta)$ for different values of δ

4. Conclusion

This study focuses on investigating the steady flow of a couple stress fluid over a deformable surface in the presence of hybrid nanoparticles and heat generation. The governing problem is transformed using similarity transformation, and the numerical solution is obtained utilizing the bvp4c solver. The findings suggest that hybrid nanofluids exhibit exceptional thermal conductivity and play a vital role in augmenting the rate of heat transfer. It is reveals that the heat transfer rate is increased by 0.78% for $\phi_{hnf} = 2\%$ and 1.61% for $\phi_{hnf} = 4\%$ if compared to $\phi_{hnf} = 0\%$ (regular fluid). Moreover, a reduction in the heat transfer rates is observed with larger heat generation parameter.

Acknowledgement

A grateful acknowledgement goes to Universiti Teknikal Malaysia Melaka, Universiti Teknologi MARA, and Universiti Kebangsaan Malaysia. This research was funded by Universiti Teknikal Malaysia Melaka (JURNAL/2019/FTKMP/Q00042).

References

[1] S.U.S. Choi, J.A. Eastman, Enhancing thermal conductivity of fluids with nanoparticles, Proceedings of the 1995 ASME International Mechanical Engineering Congress and Exposition, FED 231/MD. 66 (1995) 99–105. https://doi.org/10.1115/1.1532008.

[2] K. Khanafer, K. Vafai, M. Lightstone, Buoyancy-driven heat transfer enhancement in a two-dimensional enclosure utilizing nanofluids, Int J Heat Mass Transf. 46 (2003) 3639–3653. https://doi.org/10.1016/S0017-9310(03)00156-X.

[3] H.F. Oztop, E. Abu-Nada, Numerical study of natural convection in partially heated rectangular enclosures filled with nanofluids, Int J Heat Fluid Flow. 29 (2008) 1326–1336. https://doi.org/10.1016 /j.ijheatfluidflow.2008.04.009.

[4] S. Jana, A. Salehi-Khojin, W.H. Zhong, Enhancement of fluid thermal conductivity by the addition of single and hybrid nano-additives, Thermochim Acta. 462 (2007) 45–55. https://doi.org/10.1016/j.tca.2007.06.009.

[5] J.A.R. Babu, K.K. Kumar, S.S. Rao, State-of-art review on hybrid nanofluids, Renewable and Sustainable Energy Reviews. 77 (2017) 551–565. https://doi.org /10.1016/j.rser.2017.04.040.

[6] N.A.C. Sidik, I.M. Adamu, M.M. Jamil, G.H.R. Kefayati, R. Mamat, G. Najafi, Recent progress on hybrid nanofluids in heat transfer applications: A comprehensive review, International Communications in Heat and Mass Transfer. 78 (2016) 68–79. https://doi.org/10.1016/j.icheatmasstransfer.2016.08.019.

[7] S. Suresh, K.P. Venkitaraj, P. Selvakumar, M. Chandrasekar, Synthesis of Al2O3-Cu/water hybrid nanofluids using two step method and its thermo physical properties, Colloids Surf A Physicochem Eng Asp. 388 (2011) 41–48. https://doi.org/10.1016/j. colsurfa.2011.08.005.

[8] B. Takabi, S. Salehi, Augmentation of the heat transfer performance of a sinusoidal corrugated enclosure by employing hybrid nanofluid, Advances in Mechanical Engineering. 6 (2014) 147059. https://doi. org/10.1155/2014/147059.

[9] I. Waini, A. Ishak, I. Pop, Hybrid nanofluid flow on a shrinking cylinder with prescribed surface heat flux, Int J Numer Methods Heat Fluid Flow. 31 (2021) 1987–2004. https://doi.org/10.1108/HFF-07-2020-0470.

[10] I. Waini, A. Ishak, I. Pop, Hybrid nanofluid flow over a permeable non-isothermal shrinking surface, Mathematics. 9 (2021) 538. https://doi.org/https://doi.org/10.3390/math9050538.

[11] I. Waini, A. Ishak, I. Pop, Symmetrical solutions of hybrid nanofluid stagnation-point flow in a porous medium, International Communications in Heat and Mass Transfer. 130 (2022) 105804. https://doi.org/10.1016/j.icheatmasstransfer.2021.105804.

[12] N.S. Khashi'ie, N.M. Arifin, I. Pop, Magnetohydrodynamics (MHD) boundary layer flow of hybrid nanofluid over a moving plate with Joule heating, Alexandria Engineering Journal. 61 (2022) 1938–1945. https://doi.org/10.1016/j.aej.2021.07.032.

[13] N.S. Khashi'ie, I. Waini, A. Ishak, I. Pop, Blasius Flow over a Permeable Moving Flat Plate Containing Cu-Al2O3 Hybrid Nanoparticles with Viscous Dissipation and Radiative Heat Transfer, Mathematics 2022, Vol. 10, Page 1281. 10 (2022) 1281. https://doi.org/10.3390/MATH10081281.

[14] V.K. Stokes, Couple Stresses in Fluids, Theories of Fluids with Microstructure. (1984) 34–80. https://doi.org/10.1007/978-3-642-82351-0_4.

[15] M. Turkyilmazoglu, Exact solutions for two-dimensional laminar flow over a continuously stretching or shrinking sheet in an electrically conducting quiescent couple stress fluid, Int J Heat Mass Transf. 72 (2014)1–8. https://doi.org/10.1016/j.ijheatmasstransfer.2014.01.009.

[16] N.A. Khan, F. Riaz, N.A. Khan, Heat Transfer Analysis for Couple Stress Fluid over a Nonlinearly Stretching Sheet, Nonlinear Engineering. 2 (2013) 121–127. https://doi.org/10.1515/NLENG-2013-0014.

[17] S. Das, A. Ali, R.N. Jana, Darcy–Forchheimer flow of a magneto-radiated couple stress fluid over an inclined exponentially stretching surface with Ohmic dissipation, World Journal of Engineering. 18 (2021) 345–360. https://doi.org/10.1108/WJE-07-2020-0258/FULL/PDF.

[18] M.B. and R.T.H. M A Wahed, Potential of solar thermal system for industrial process heat applications in the tropics, Alam Cipta, UPM. 8 (2015).

[19] D. Schüwer, C. Schneider, Electrification of industrial process heat: Long-term applications, potentials and impacts, in: Eceee Industrial Summer Study Proceedings, 2018.

[20] N. Tasmin, S.H. Farjana, M.R. Hossain, S. Golder, M.A.P. Mahmud, Integration of Solar Process Heat in Industries: A Review, Clean Technologies. 4 (2022). https://doi.org/10.3390/cleantechnol4010008.

[21] Y. Liu, W. Chen, D. Jiang, Review on Heat Generation of Rubber Composites, Polymers (Basel). 15 (2023). https://doi.org/10.3390/polym15010002.

[22] O.D. Makinde, P.O. Olanrewaju, Combined effects of internal heat generation and buoyancy force on boundary layer flow over a vertical plate with a convective surface boundary condition, Canadian Journal of Chemical Engineering. 90 (2012). https://doi.org/10.1002/cjce.20614.

[23] M.I. Khan, T. Hayat, M. Waqas, M.I. Khan, A. Alsaedi, Impact of heat generation/absorption and homogeneous-heterogeneous reactions on flow of Maxwell fluid, J Mol Liq. 233 (2017). https://doi.org/10.1016/j.molliq.2017.03.049.

[24] O. Ojjela, N. Naresh Kumar, D.R.V.S.R.K. Sastry, Radiation and Heat Generation Effects on Couple Stress Fluid Through Expanding Channel, in: Lecture Notes in Mechanical Engineering, 2021. https://doi.org/10.1007/978-981-15-4308-1_69.

[25] W. Ibrahim, G. Gadisa, Finite element solution of nonlinear convective flow of Oldroyd-B fluid with Cattaneo-Christov heat flux model over nonlinear stretching sheet with heat generation or absorption, Propulsion and Power Research. 9 (2020). https://doi.org/10.1016/j.jppr.2020.07.00.

[26] B. Shankar Goud, Heat generation/absorption influence on steady stretched permeable surface on MHD flow of a micropolar fluid through a porous medium in the presence of variable suction/injection , International Journal of Thermofluids. 7–8 (2020). https://doi.org/10.1016/j.ijft.2020.100044.

[27] A. Adeniyan, F. Mabood, S.S. Okoya, Effect of heat radiating and generating second-grade mixed convection flow over a vertical slender cylinder with variable physical properties, International Communications in Heat and Mass Transfer. 121 (2021).

https://doi.org/10.1016/j.icheatmasstransfer.2021.105110.

[28] I. Tlili, H.A. Nabwey, G.P. Ashwinkumar, N. Sandeep, 3-D magnetohydrodynamic AA7072-AA7075/methanol hybrid nanofluid flow above an uneven thickness surface with slip effect, Sci Rep. 10 (2020) 1–13. https://doi.org/10.1038/s41598-020-61215-8.

[29] L.F. Shampine, I. Gladwell, S. Thompson, Solving ODEs with MATLAB, Cambridge University Press, Cambridge, 2003. https://doi.org/https://doi.org/10.1017/cbo9780511615542.